Supporting Information

SNARE zippering requires activation by SNARE-like peptides in Sec1/Munc18 proteins

Haijia Yu[1,2], Chong Shen[2], Yinghui Liu[1,2], Bridget L. Menasche[2], Yan Ouyang[2],

Michael H. B. Stowell[2,3*], and Jingshi Shen[2*]

[1]Jiangsu Key Laboratory for Molecular and Medical Biotechnology, College of Life Sciences, Nanjing Normal University, Nanjing, 210023, China.

[2]Department of Molecular, Cellular and Developmental Biology, University of Colorado Boulder, Boulder, CO 80309, USA.

[3]Department of Mechanical Engineering, University of Colorado Boulder, Boulder, CO 80309, USA.

*Correspondence: michael.stowell@colorado.edu (M.S.); jingshi.shen@colorado.edu (J.S.)

This file includes:

Additional characterization of SLP function

Figures S1 to S14

Table S1

Additional characterization of SLP function

It was previously shown that Vn peptide (corresponding to the NTD of the v-SNARE) inhibits SNARE-mediated membrane fusion (*1, 2*). We observed that Vn also inhibited the basal liposome fusion reactions driven by the VAMP2-SLP chimera, in which the CTD of VAMP2 was replaced with the SLP of Munc18-1, or VAMP2 mutants with +1 or +2 layer deletion (Fig. S12). These results suggest that the N-to-C assembly pathway of SNAREs is not altered by SLP substitution or deletion of +1 or +2 layer. We then examined how Munc18-1 regulates the fusion reaction driven by the VAMP2-SLP chimera. We observed that Munc18-1 failed to stimulate this fusion reaction (Fig. S13). This finding is expected because the stimulation of fusion by Munc18-1 requires surface residues in VAMP2 CTD and these surface residues are absent in the SLP sequence (*3, 4*). Finally, we examined the regulatory activity of the Munc18-1-Vc chimera in which the SLP sequence of Munc18-1 was replaced with VAMP2 CTD. We observed that the Munc18-1-Vc chimera did not activate SNARE-dependent liposome fusion (Fig. S14). In fact, it markedly inhibited the fusion kinetics (Fig. S14). These data are consistent with our observation that Vc is intrinsically stronger than SLP in SNARE binding (Fig. 6). In the context of full-length Munc18-1, the binding of Vc peptide to t-SNAREs is further augmented by non-SLP binding modes of Munc18-1. As a result, Vc peptide (within Munc18-1 protein) cannot be efficiently displaced by full-length v-SNARE, leading to fusion inhibition. These results further support the notion that SLP recognizes t-SNARE CTDs during the fusion reaction.

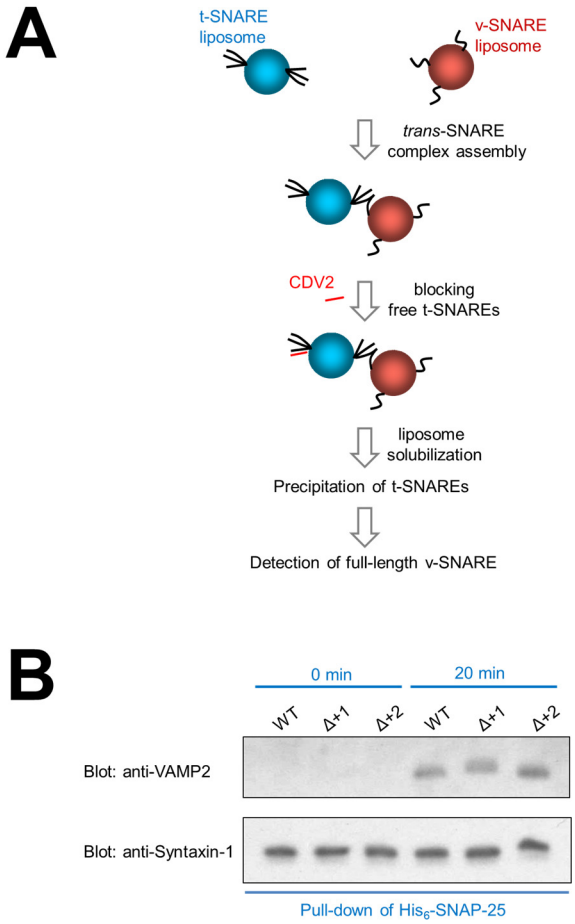

Figure S1. Deletion of the +1 or +2 layer of VAMP2 does not alter the assembly of trans-SNARE complex. (A) Illustration of the trans-SNARE assembly assay. Reconstituted t- and v-SNARE liposomes were incubated at 4 ºC for the indicated time periods before 10-fold excess amount of inhibitory VAMP2 CD (CDV2) was added to block unpaired t-SNAREs. The liposomes were subsequently solubilized and the t-SNAREs were precipitated using nickel sepharose beads. Presence of full-length VAMP2 in the precipitates was probed by immunoblotting, which was used as an indicator for trans-SNARE assembly between liposomes. The reactions were performed in the presence of 100 mg/mL Ficoll 70. **(B)** Immunoblots showing syntaxin-1 and VAMP2 protein levels in the precipitates from the trans-SNARE assembly assays.

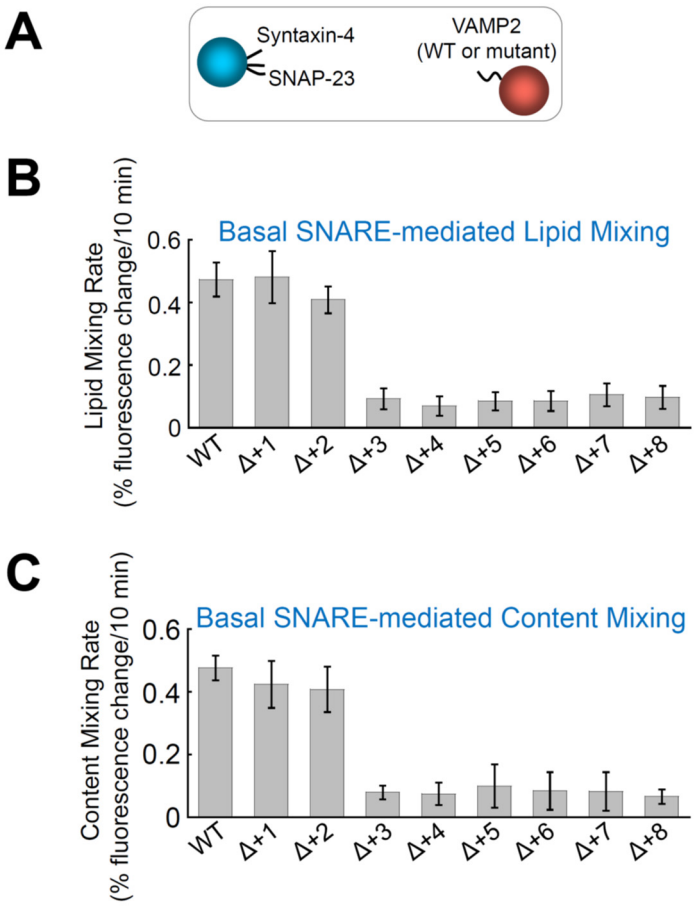

Figure S2. The +1 and +2 layers of the v-SNARE are dispensable for the basal fusion reaction mediated by GLUT4 exocytic SNAREs. (A) Illustration of the liposome fusion pairs. The GLUT4 exocytic t-SNARE liposomes were reconstituted using syntaxin-4 and SNAP-23, whereas the v-SNARE liposomes contained WT or mutant VAMP2. **(B)** Initial lipid-mixing rates of the liposome fusion reactions reconstituted with WT t-SNAREs and WT or mutant VAMP2. Liposome fusion reactions were carried out as in Figure 1B. Each fusion reaction contained 5 μM t-SNAREs, 1.5 μM v-SNARE, and 100 mg/mL Ficoll 70. **(C)** Initial rates of content mixing of the reconstituted fusion reactions. The v-SNARE liposomes, in which sulforhodamine B was encapsulated, were directed to fuse with unlabeled t-SNARE

liposomes. Data in B and C are presented as percentage of fluorescence change per 10 min. Error bars indicate standard deviation.

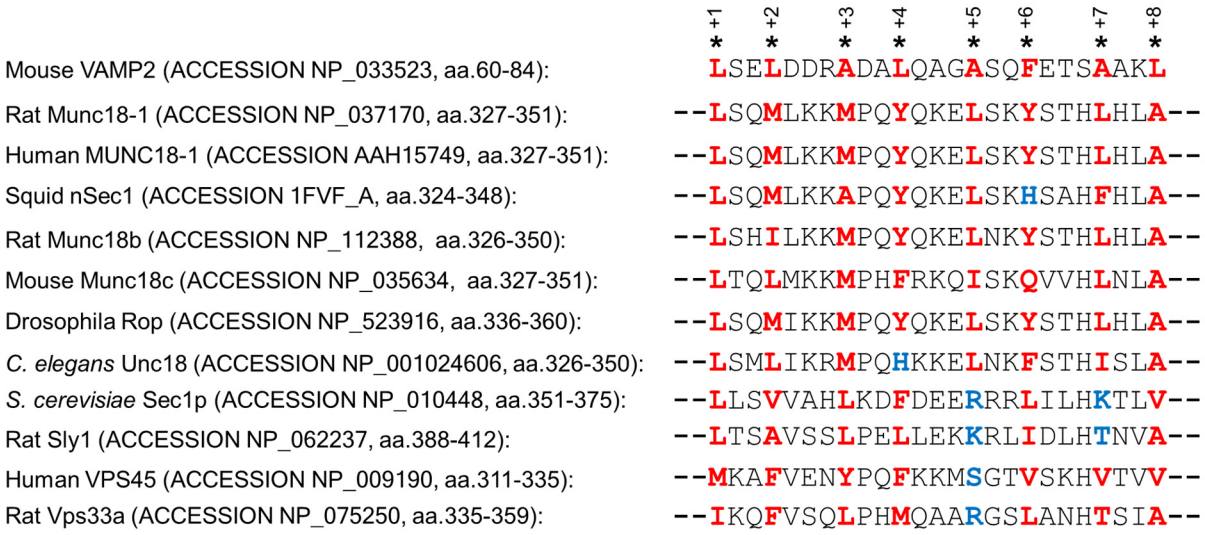

Figure S3. Alignment of VAMP2 CTD with SLP sequences from SM proteins. The COBALT program (https://www.ncbi.nlm.nih.gov/tools/cobalt/re_cobalt.cgi) was used to perform an unbiased alignment between VAMP2 CTD (aa. 60-84) and 11 full-length SM proteins. In the alignment, Word Size was set to 3, End Gap Open Penalty was set to -1, Max Cluster Distance was set to 0.95, and other parameters were set to default. The SLPs are the only SM protein sequences exhibiting similarity to VAMP2 CTD in this alignment. The layer residues of VAMP2 CTD are numbered and indicated with asterisks. The hydrophobic layer-like residues of SLP sequences are shown in red with exceptions shown in blue.

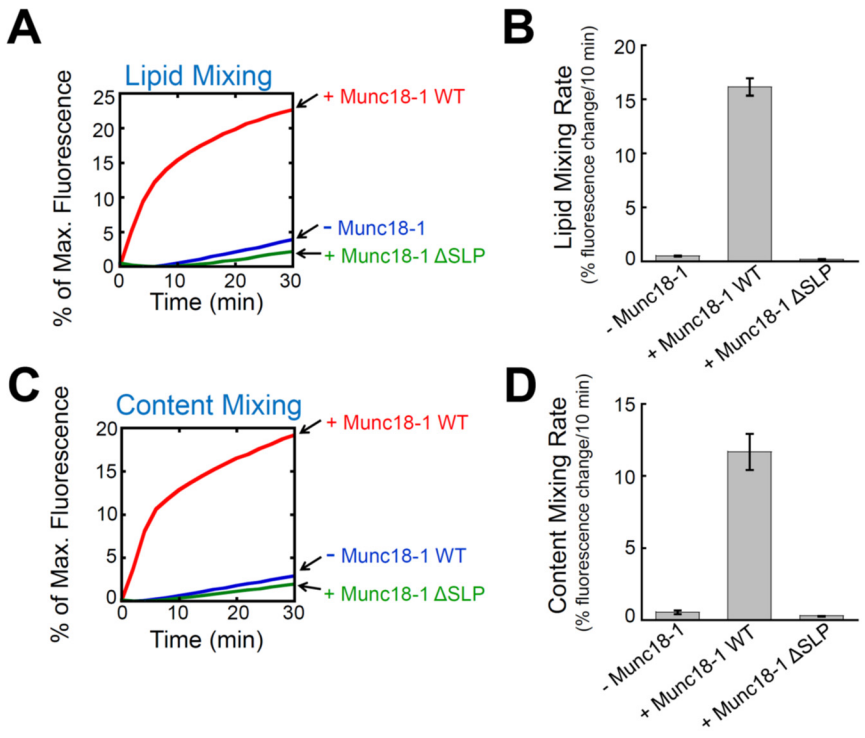

Figure S4. SLP is required for the stimulatory function of Munc18-1. (A) Lipid mixing of the reconstituted fusion reactions in the absence or presence of WT or SLP (a.a. 327-351)-deficient Munc18-1. Liposome fusion reactions were carried out as in Figure 1B. **(B)** Initial lipid-mixing rates of the reconstituted fusion reactions shown in A. Data are presented as percentage of fluorescence change per 10 min. Error bars indicate standard deviation. **(C)** Content mixing of the reconstituted fusion reactions in the absence or presence of WT or SLP-deficient Munc18-1. Liposome fusion reactions were carried out as in Figure 1C. **(D)** Initial content-mixing rates of the reconstituted fusion reactions shown in C. Data are presented as percentage of fluorescence change per 10 min. Error bars indicate standard deviation.

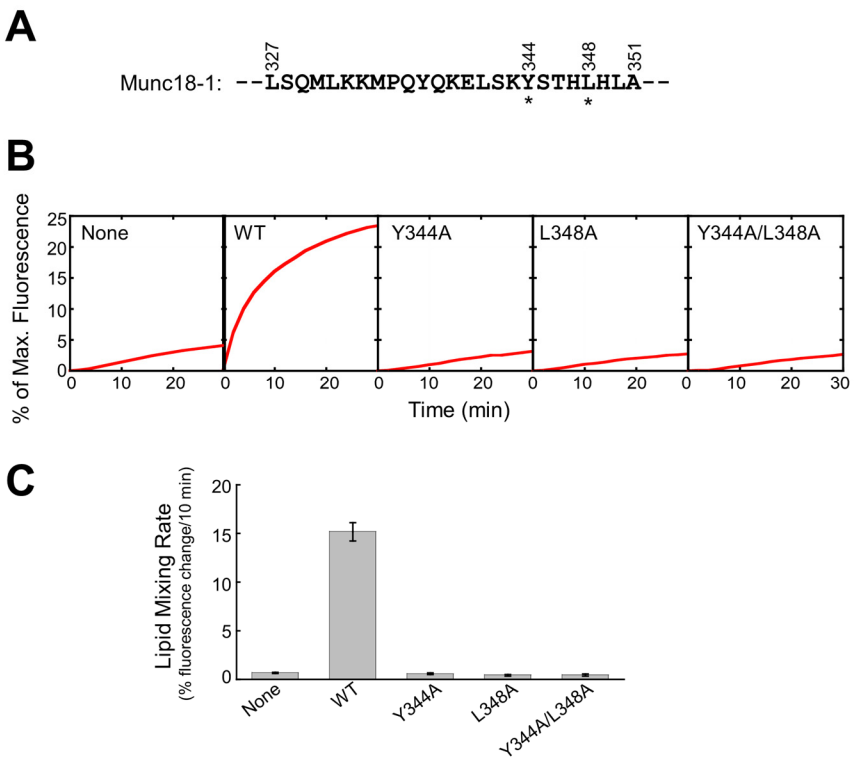

Figure S5. Mutations of layer-like residues in SLP abrogate the stimulatory function of Munc18-1. (A) Sequence of Munc18-1 SLP with mutated residues highlighted by asterisks. As shown in Figure 4A, Y344 is aligned to the +6 layer of VAMP2 whereas L348 is aligned to the +7 layer of VAMP2. **(B)** Lipid mixing of the reconstituted fusion reactions in the absence or presence of 5 μM WT or mutant Munc18-1 proteins. Liposome fusion reactions were carried out as in Figure 1B. **(C)** Initial lipid-mixing rates of the reconstituted fusion reactions shown in B. Data are presented as percentage of fluorescence change per 10 min. Error bars indicate standard deviation.

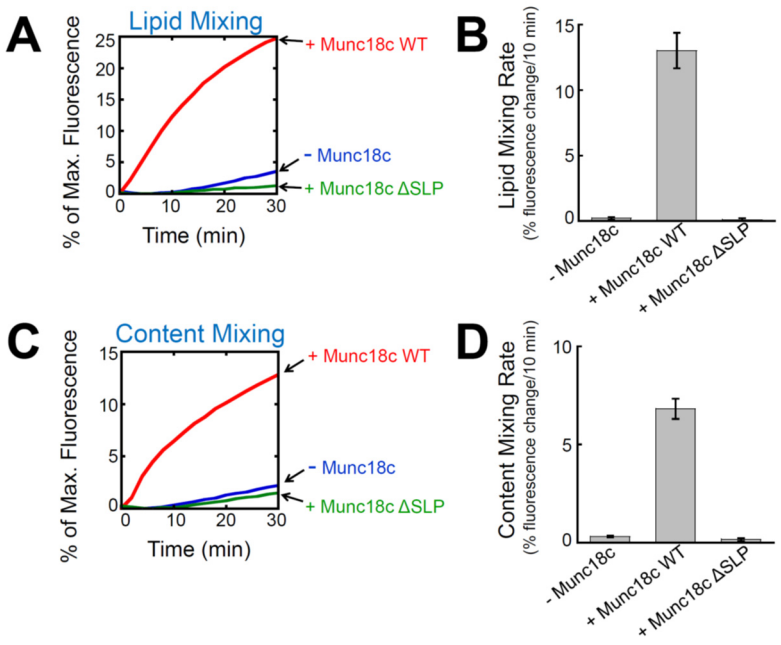

Figure S6. SLP is crucial to the stimulatory activity of Munc18c. (A) Lipid mixing of the reconstituted fusion reactions in the absence or presence of WT or SLP (a.a. 327-351)-deficient Munc18c. Liposome fusion reactions were carried out as in Figure 1B. **(B)** Initial lipid-mixing rates of the reconstituted fusion reactions shown in A. Data are presented as percentage of fluorescence change per 10 min. Error bars indicate standard deviation. **(C)** Content mixing of the reconstituted fusion reactions in the absence or presence of WT or SLP-deficient Munc18c proteins. Liposome fusion reactions were carried out as in Figure 1C. **(D)** Initial content-mixing rates of the reconstituted fusion reactions shown in C. Data are presented as percentage of fluorescence change per 10 min. Error bars indicate standard deviation.

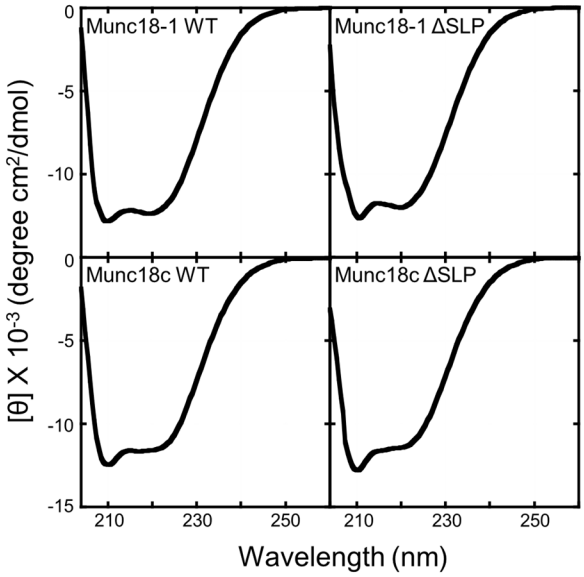

Figure S7. Circular dichroism (CD) spectroscopic analysis of WT and mutant SM proteins. The CD spectra were measured using a Jasco J-815 spectropolarimeter equipped with a 1 mm quartz cell. The readings were made at 0.5 nm intervals, and each data point represented the average of six scans at a speed of 50 nm/min over the wavelength range of 200 nm to 260 nm. The data were converted into mean residue weighted molar ellipticity using the following equation: $[\theta]_{\mathrm{MRW}} = (100 \times \theta)/Cnl$, where C is the protein concentration (mM), θ is the measured ellipticity (milli-degree), n is the number of residues, and l is the path length (cm).

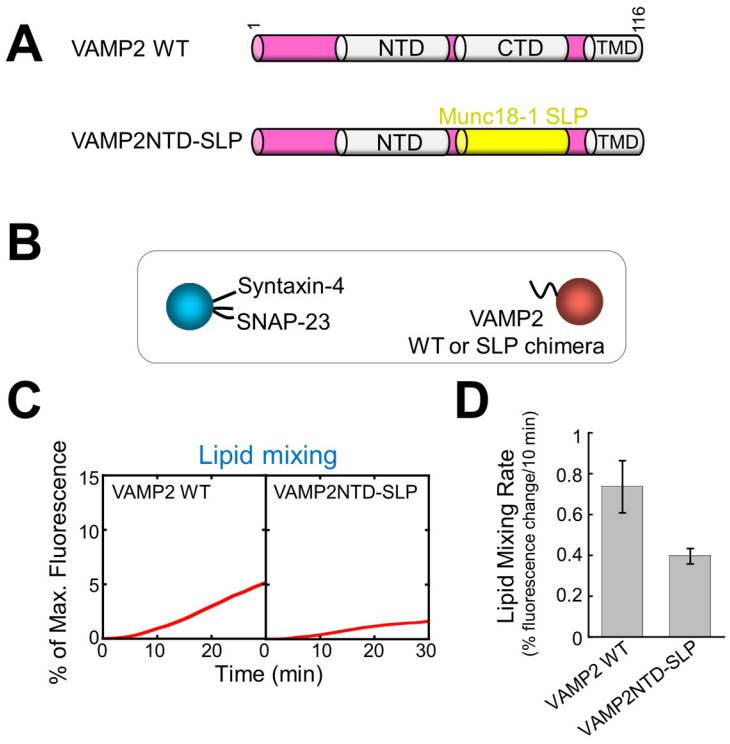

Figure S8. The selectivity of Munc18-1 SLP in driving membrane fusion. (A) Diagrams of WT VAMP2 and VAMP2-SLP chimera. SLP corresponds to aa. 327-351 of Munc18-1. The sequence of the chimera is included in Methods. **(B)** Illustration of the liposome fusion pairs. **(C)** Lipid mixing of the reconstituted fusion reactions described in B. Liposome fusion reactions were carried out as in Figure 1B. **(D)** Initial lipid-mixing rates of the reconstituted fusion reactions in C. Data are presented as percentage of fluorescence change per 10 min. Error bars indicate standard deviation.

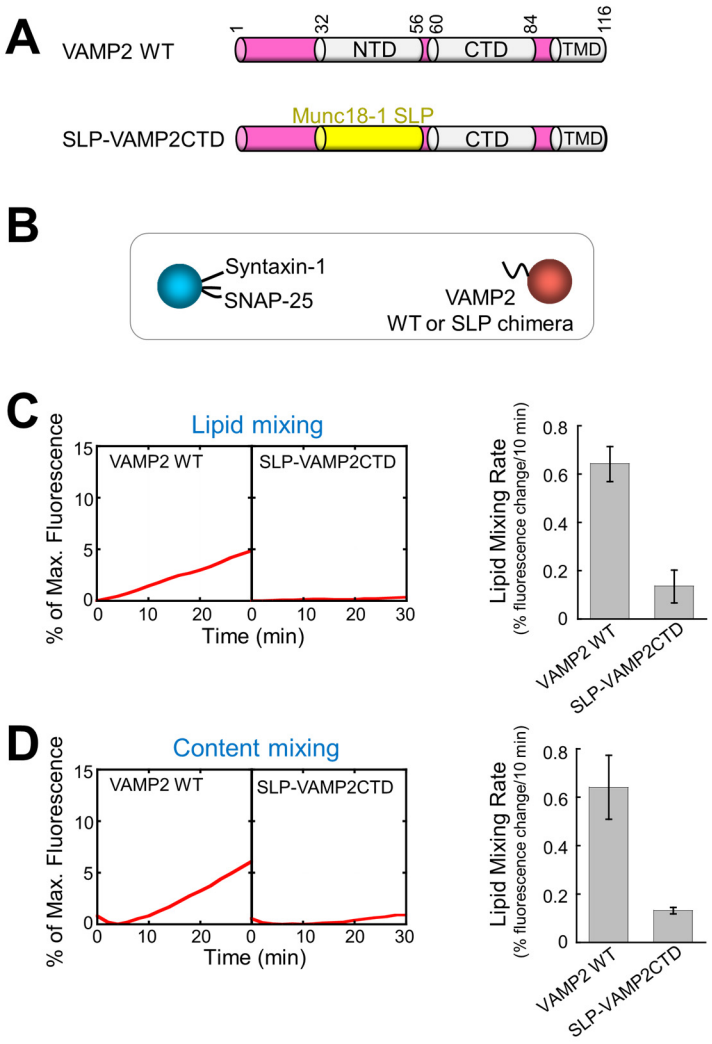

Figure S9. SLP is unable to replace v-SNARE NTD in driving membrane fusion. (A) Diagrams of WT VAMP2 and SLP-VAMP2 chimera. SLP corresponds to aa. 327-351 of Munc18-1. The sequence of the chimera is included in Methods. **(B)** Illustration of the liposome fusion pairs. **(C)** Left: lipid mixing of the reconstituted fusion reactions described in B. Right: initial lipid-mixing rates of the reconstituted fusion reactions. Liposome fusion reactions were carried out as in Figure 1B. Data are presented as percentage of fluorescence change per 10 min. Error bars indicate standard deviation. **(D)** Left: content mixing of the reconstituted fusion reactions described in B. Right: initial content-mixing rates of the reconstituted fusion reactions. Liposome fusion reactions were carried out as in Figure 1C.

Data are presented as percentage of fluorescence change per 10 min. Error bars indicate standard deviation.

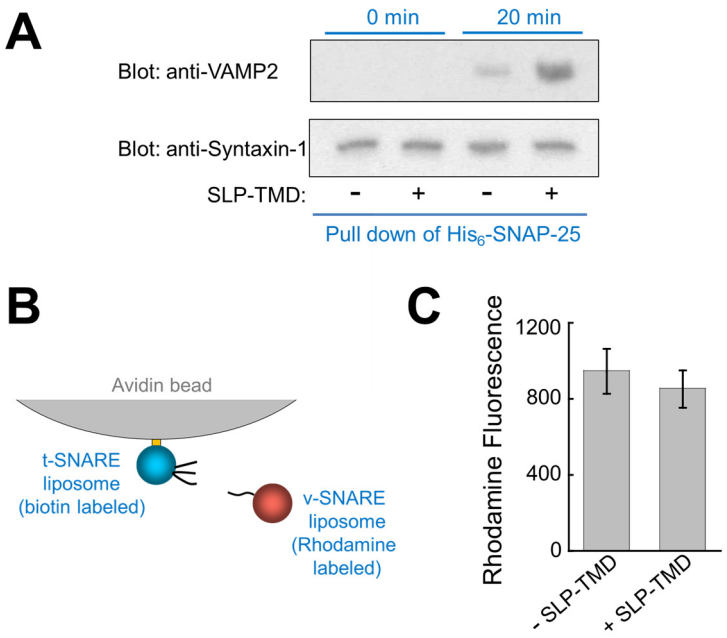

Figure S10. SLP does not promote the initial docking of SNARE liposomes. (A) Stimulation of trans-SNARE assembly by SLP-TMD. The trans-SNARE assembly assay was performed as described in Figure S1. SLP-TMD was reconstituted in the t-SNARE liposomes. SLP-TMD is illustrated in Figure 6A and its sequence is included in Methods. **(B)** The liposome docking assay was performed as previously described (*5*). The biotin-labeled t-SNARE liposomes containing syntaxin-1 and SNAP-25 were anchored to avidin beads and used to pull down rhodamine-labeled v-SNARE liposomes reconstituted using the VAMP2NTD-TolA chimera. Depicted in Figure 4C, the VAMP2NTD-TolA chimera was used here to selectively monitor the upstream docking step. The binding reactions were performed at 4 ºC for one hour in the absence or presence of SLP-TMD anchored in the t-SNARE liposomes. **(C)** Effects of SLP-TMD on liposome docking. Data are presented as rhodamine fluorescence intensity. The binding reaction containing protein-free liposomes was used as a negative control to obtain the background fluorescence signal. The background rhodamine

fluorescence was subtracted from other binding reactions to reflect specific SNARE-dependent liposome docking. Error bars indicate standard deviation.

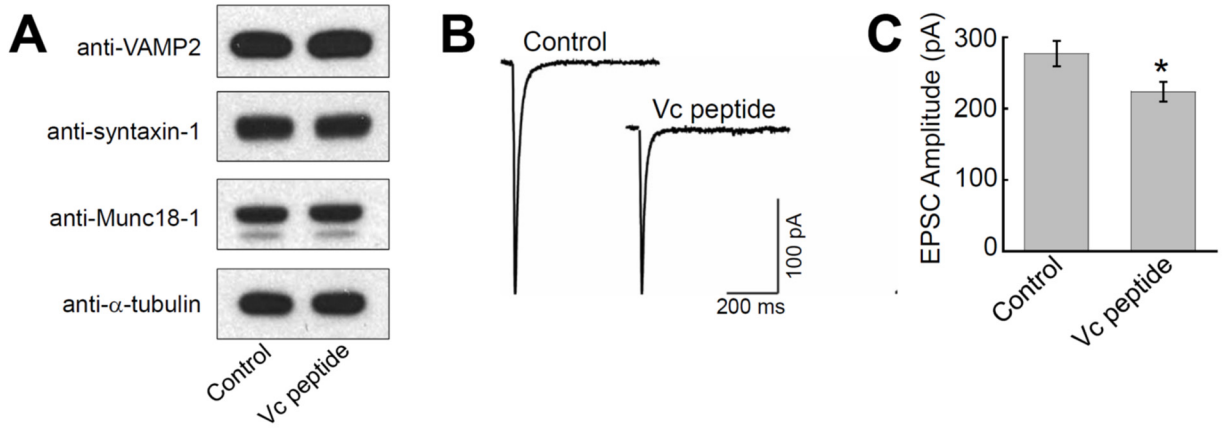

Figure S11. Evoked synaptic exocytosis is reduced in Vc peptide-expressing neurons. (A) Immunoblots showing the expression of the indicated proteins in the cultured neurons. **(B)** Representative traces of excitatory postsynaptic currents (EPSCs) evoked by local electrical stimulation in cultured neurons. **(C)** Summary graph of EPSC amplitudes. Numbers of neurons and independent cultures are listed in Table S1. **P*<0.05.

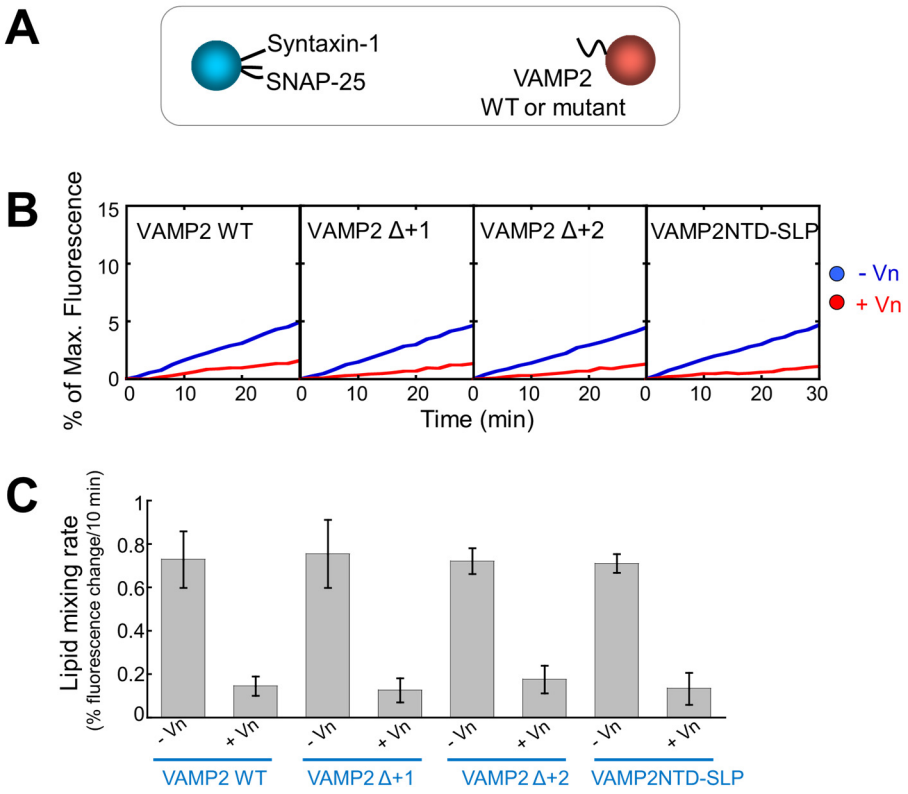

Figure S12. Vn peptide inhibits fusion reactions mediated by WT or mutant SNAREs. **(A)** Illustration of the liposome fusion pairs. **(B)** Lipid mixing of the reconstituted fusion reactions described in A. Liposome fusion reactions were carried out as in Figure 1B with or without 5 μM Vn peptide (aa. 28-57 of VAMP2). **(C)** Initial lipid-mixing rates of the reconstituted fusion reactions shown in B. Data are presented as percentage of fluorescence change per 10 min. Error bars indicate standard deviation.

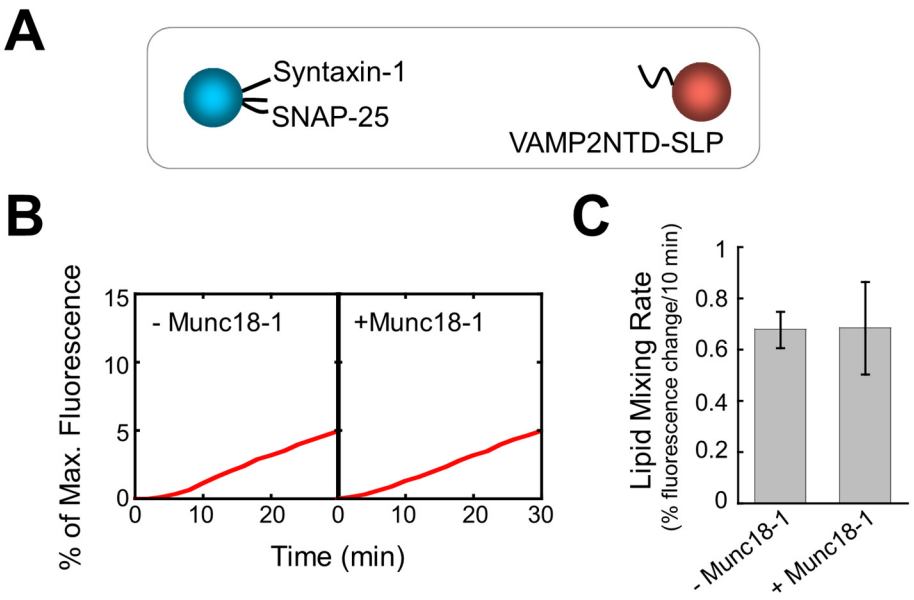

Figure S13. Munc18-1 does not stimulate the fusion reaction containing the VAMP2-SLP chimera. (A) Illustration of the liposome fusion pairs. **(B)** Lipid mixing of the reconstituted fusion reactions described in A. Liposome fusion reactions were carried out as in Figure 1B with or without 5 μM Munc18-1. **(C)** Initial lipid-mixing rates of the reconstituted fusion reactions shown in B. Data are presented as percentage of fluorescence change per 10 min. Error bars indicate standard deviation.

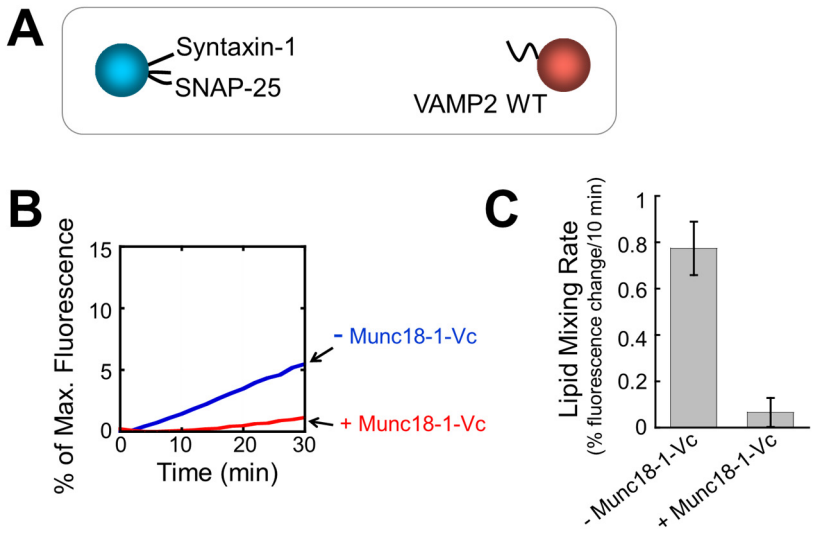

Figure S14. Munc18-1-Vc chimera inhibits SNARE-mediated membrane fusion. (A) Illustration of the liposome fusion pairs. **(B)** Lipid mixing of the reconstituted fusion reactions described in A. Liposome fusion reactions were carried out as in Figure 1B with or without Munc18-1-Vc chimera (5 μM), in which the SLP of Munc18-1 was replaced with VAMP2 CTD. The sequence of the Munc18-1-Vc chimera is included in Methods. **(C)** Initial lipid-mixing rates of the reconstituted fusion reactions shown in B. Data are presented as percentage of fluorescence change per 10 min. Error bars indicate standard deviation.

Table S1
Summary of Electrophysiological Data

Figure / Analyzed group	Analyzed parameter (unit) / Value (means±SEMs)	Number of cultures	Total number of neurons	*p* Value (Student's t-test)
Figure 7				
	mEPSC frequency (Hz)			
Control	12.50±1.18	4	31	
Vc peptide	8.12±0.90	4	31	<0.01
	mEPSC amplitude (pA)			
Control	24.08±0.97	4	31	
Vc peptide	24.87±1.51	4	31	n.s.
Figure S6				
	EPSC amplitude (pA)			
Control	277.06±17.88	4	22	
Vc peptide	223.69±13.63	4	23	<0.05

n.s.: not significant

References

1. F. Li *et al.*, A half-zippered SNARE complex represents a functional intermediate in membrane fusion. *J Am Chem Soc* **136**, 3456-3464 (2014).
2. T. J. Melia *et al.*, Regulation of membrane fusion by the membrane-proximal coil of the t-SNARE during zippering of SNAREpins. *The Journal of cell biology* **158**, 929-940 (2002).
3. C. Shen *et al.*, The trans-SNARE-regulating function of Munc18-1 is essential to synaptic exocytosis. *Nat Commun* **6**, 8852 (2015).
4. J. Shen, D. C. Tareste, F. Paumet, J. E. Rothman, T. J. Melia, Selective Activation of Cognate SNAREpins by Sec1/Munc18 Proteins. *Cell* **128**, 183-195 (2007).

5. H. Yu *et al.*, Comparative studies of Munc18c and Munc18-1 reveal conserved and divergent mechanisms of Sec1/Munc18 proteins. *Proc Natl Acad Sci U S A* **110**, E3271-3280 (2013).